Facile synthesis and high d_{33} of single-crystalline $KNbO_3$ nanocubes†

Haiyan Ge, Yudong Hou,* Mankang Zhu, Hao Wang and Hui Yan

Received (in Cambridge, UK) 19th June 2008, Accepted 11th July 2008
First published as an Advance Article on the web 8th September 2008
DOI: 10.1039/b810342a

Single-crystalline $KNbO_3$ nanocubes with orthorhombic phase were prepared in a large scale by a simple one-step molten salt route without using any surfactant as template; the nanostructures exhibited high piezoelectric properties such as d_{33} = 105 pC/N and k_p = 0.34 as piezoelectric materials.

Much attention has been paid to environmental preservation worldwide in recent years. In the research field of piezoelectric ceramics, there is an increasing strong demand to develop alternative lead-free piezoelectric materials against PZT based compounds. Potassium niobate ($KNbO_3$; KN) ceramics have received considerable interest as a candidate material for lead-free piezoelectric applications, because single-crystal KN has a large piezoelectricity and a high Curie point of 435 °C.[1,2] The electromechanical coupling factor of the thickness-extensional mode k_t, in a KN crystal reaches as high as 0.69 for the 49.5° rotated *X*-cut about the *Y*-axis, which is the highest among current lead-free piezoelectrics.[3]

Unfortunately, pure $KNbO_3$ is difficult to synthesize by conventional methods as a mechanically robust, high-density, nondeliquescent ceramic, which limits our knowledge of the piezoelectricity of this ceramic. The problems typically encountered include K loss, porosity and microcracking, in extreme cases leading to spontaneous fracture. Since important ceramic physical properties such as sintered density, chemical homogeneity, and piezoelectric properties are affected by the final crystallite powder,[4] much attention has been devoted to the synthesis of KN powders using different methods. For obtaining potassium niobate powders, methods have been used such as hydrothermal synthesis,[5] a glycothermal technique,[6] synthesis from metal alkoxides,[7] sol–gel processes,[8] and the use of polymeric precursors (the Pechini method),[9] besides the traditional solid-state reaction of mixed oxides.[10] In all these methods, complex solution processes, toxic precursors and calcination at more or less high temperature were needed to obtain pure crystallized ferroelectric $KNbO_3$, involving the formation of hard aggregates, which are unfavorable for sintering. Therefore, the development of gram scale and environmentally friendly synthetic methods[11,12] with reproducible shape control and absence of surfactant are of paramount importance for the possibility of producing well-dispersed and highly sintering-active $KNbO_3$ nanostructures. In the present work, a large-scale and facile molten salt synthetic method is presented to produce $KNbO_3$ nanostructures in KCl by rapid sintering and quenching to room temperature in air. The piezoelectric properties are much enhanced for the $KNbO_3$ prepared by the present method.

In a typical synthesis, analytical grade K_2CO_3 (99.0%) and Nb_2O_5 (99.0%) were used as the starting materials, and KCl (99.5%) served as molten salt medium because of its low melting temperature (770 °C) and for not introducing impurity cations. First, K_2CO_3, Nb_2O_5 and KCl were mixed in a molar ratio of 1 : 1 : 6 and ground for 24 h by ball milling in ethanol medium. Before placing in an alumina crucible, the mixtures were pretreated at 120 °C for 6 h. The obtained dry mixtures were heated with a rapid rate of 8 °C min^{-1} up to 800 °C, kept at that temperature for 4 h in air, and subsequently quenched to room temperature. Pure $KNbO_3$ product was obtained after washing the quenched material several times with hot distilled water to remove the KCl. For the measurements of piezoelectric properties, the obtained nanostructures were pressed into pellets, and then sintered at 1060 °C for 2 h to achieve a high density above 97%. The sintering temperature was very close to the melting point; therefore, very careful temperature control was required during the sintering. The morphology and structure of the materials were characterized by scanning electron microscopy (SEM, Hitachi S-3500), transmission electron microscopy (TEM, JEOL-JEM 2000F), field emission high-resolution transmission electron microscopy (HRTEM, JEOL 2100F), selected area electron diffraction (SAED) and X-ray diffraction (XRD, Bruker D8). The piezoelectric coefficient d_{33} for electrically poled (3 kV mm^{-1}) disks was determined using a d_{33} tester (ZJ-2), the electromechanical coupling factor k_p was measured on a precision impedance analyzer (Agilent 4294A), and the *P*–*E* hysteresis loop was obtained by a ferroelectric tester (TF2000).

Fig. 1(a) shows the XRD pattern recorded at room temperature and the Rietveld refinement profile carried out by the software MDI jade 5.0 for the $KNbO_3$ powder generated from the current molten salt method, which exhibits sharp diffraction peaks indicating that the samples are well crystallized. The pattern, with a final weighted residue factor R_{wp} of 8.74% was refined in the orthorhombic space group *Cm*2*m* (no. 38). All of the diffraction peaks can be assigned to the orthorhombic phase of $KNbO_3$ (JCPDS 32-0822) with the refined lattice parameters of a = 5.693, b = 5.720 and c = 3.973 Å, indicating phase purity of

Department of Materials Science and Engineering, Beijing University of Technology, Beijing, 100124, People's Republic of China. E-mail: ydhou@bjut.edu.cn; Fax: +86-10-67392445; Tel: +86-10-67392445

† Electronic supplementary information (ESI) available: FT-IR spectra, Raman spectra, temperature dependence of ε_r and tan δ at various frequencies and frequency dependence of impedance on the (p) mode of the piezoelectric materials and SEM of the starting material Nb_2O_5. See DOI: 10.1039/b810342a

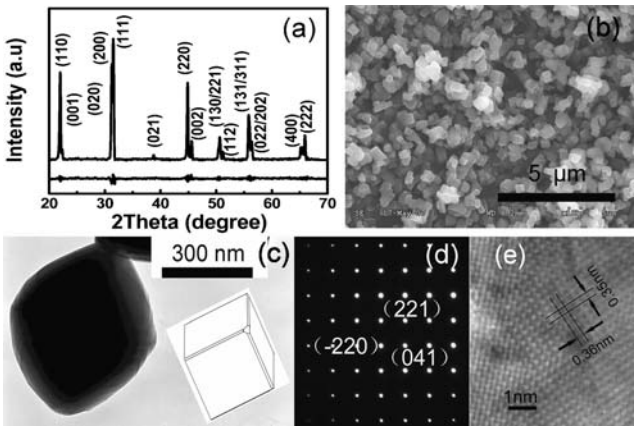

Fig. 1 (a) Rietveld refinement fit for $KNbO_3$ powder, (b) SEM image, (c) a representative individual $KNbO_3$ nanostructure with the inset showing a schematic of the facets of an individual cube, (d) selected area electron diffraction (SAED) pattern of a representative individual crystal, and (e) HRTEM image of a single-crystalline nanocube for $KNbO_3$.

the product. The FT-IR spectrum (see ESI, Fig. S1†) indicates the nonexistence of impurity Cl^- species on the surface of the nanostructures which shows only absorbed water and surface hydroxyls. In the low-wavenumber region, a broad and strong band appears around 600 cm^{-1}, which could be ascribed to the characteristic vibration of the Nb–O octahedron and indicates the formation of the perovskite phase. The Raman spectra of the $KNbO_3$ nanostructures at room temperature (see ESI, Fig. S2†) clearly shows three characteristic major bands centered at around 281, 586 and 833 cm^{-1}, which were assigned to the characteristic lattice vibration of orthorhombic $KNbO_3$, and were in good agreement with the XRD data. A typical scanning electron microscopy (SEM) image of the reaction product is shown in Fig. 1(b). The image clearly shows that the as-prepared products were free of hard agglomeration, consisting of similar cubic structures with an average size of $\sim$300 nm. Fig. 1(c) shows a representative individual $KNbO_3$ nanostructure with truncated edges which can be schematically described by the illustration shown in the inset. Selected-area electron diffraction (SAED) data (Fig. 1(d)) taken from individual cubes show the presence of sharp diffraction spots indicating the formation of well-developed, single-crystalline $KNbO_3$. We note that the electron diffraction patterns obtained from different areas of the cube also show similar sharp diffraction spots. The SAED pattern was indexed with space group *Cm*2*m* (no. 38), which is in agreement with the presently studied XRD result and the literature data (JCPDS 32-0822). Further, a high-resolution TEM (HRTEM) image reveals the nature of the single-crystalline $KNbO_3$ nanostructure in Fig. 1(e). The interplanar spacings of about 0.36 and 0.35 nm correspond to (130) and (112), respectively.

Because of the small diffusion distances of oxide mixtures in molten salts, the high reactivity of salts, and the high mobility of species, completed reactions can be achieved in a relatively short time.[13,14] Hence, single-crystalline $KNbO_3$ nanostructures have been prepared with a simple molten salt synthetic method in the presence of KCl in our case. Upon heating of the initial mixture, the precursor K_2CO_3 dissolved into the resultant molten flux, whereas the other precursor Nb_2O_5 is insoluble in alkali-metal chlorides, and gradually formed $KNbO_3$ at the surface of the Nb_2O_5 particles, which itself has very limited solubility, implying that a ''template formation'' mechanism plays a crucial role.[13,15,16] In our case, the fact that the cubic morphologies of $KNbO_3$ were similar to those of the starting Nb_2O_5 material (see ESI, Fig. S3†) confirmed the ''template formation'' mechanism.

Due to the good sinterability and pure perovskite structure of nanosize powders,[17] the $KNbO_3$ nanostructures synthesized by the molten salt synthetic method were selected to prepare ceramics. The pressed pellets made by nanostructures show $>$97% theoretical density at 1060 °C for 2 h. It is believed that the relative density of a sintered ceramic is directly related to the green density of the pressed pellets (meaning the density of the pressed pellets before sintering), which in turn is highly dependent on the morphology of the precursor oxide powders.[18] As seen in Fig. 1, the powder synthesized by the molten salt synthetic method gives free-standing $KNbO_3$ nanostructures. The freestanding nanostructures have a high packing efficiency and therefore a high green density of about 65% of the theoretical density, which is responsible for the high densification during sintering. However, powders synthesized by conventional methods have a green density of only about 56% of the theoretical density. In addition, smaller nanostructures with high surface to volume ratio should contain more surface oxygen vacancies, which enhance the transfer of mass and energy between reactants, thus improving the sintering behavior.[19]

During the sintering process, the highly volatile K_2O limits stoichiometric control of $KNbO_3$ ceramics.[10,20] This serious problem restricted $KNbO_3$ ceramics from fully densifying and lead the appearance of an unstable impurity phase, $K_4Nb_6O_{17}$, which displays deliquescence when exposed to humidity. Fig. 2(a) reveals the top external view of a $KNbO_3$ ceramic disk ($<$90% of

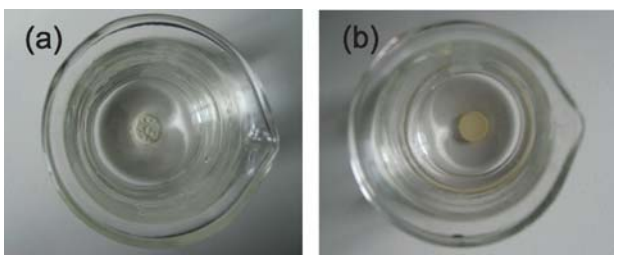

Fig. 2 Top external view of $KNbO_3$ ceramic disks just after immersion into water. The disks were sintered (a) by ordinary ceramic processing and (b) with $KNbO_3$ nanostructures derived from the molten salt synthetic method by pressureless sintering.

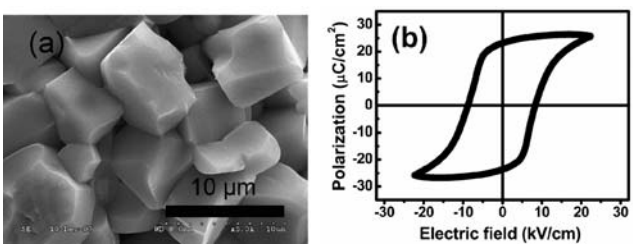

Fig. 3 (a) SEM micrographs of cross sections of $KNbO_3$ ceramic and (b) *P*–*E* hysteresis loop of $KNbO_3$ ceramics.

Table 1 Piezoelectric properties of KN systems cited from several previous reports

Composition	Ref.	d_{33} (pC/N)	k_p	E_c/kV cm^{-1}	P_r/μC cm^{-2}	Method
$KNbO_3$	This study	105	0.34	8	23	OF
$KNbO_3$	10	—	0.25	15.5	14	OF (O_2 rich atmosphere)
$KNbO_3$	21	66.4	—	18	23	OF
$KNbO_3$	22	91.7	0.28	—	—	OF
$KNbO_3$–0.002 $LaFeO_3$	23	98	0.17	9	18	OF (O_2 rich atmosphere)
$KNbO_3$–0.01 Co	24	—	0.16	16	14	OF

OF = ordinary furnace.

theoretical density) sintered by a standard ceramic processing used for oxide ferroelectrics. When the disk was immersed in water, it immediately demonstrated a highly hygroscopic behavior. The sintered body showed rapid disintegration and dissolved in water with evidence of decomposition. In contrast, the disk prepared by our new method demonstrated no reaction under water as shown in Fig. 2(b). Therefore, $KNbO_3$ nanostructures synthesized by the molten salt synthetic method play an important role in acquiring "water-proof" ceramics.

Fig. 3(a) shows SEM micrographs of cross sections of $KNbO_3$ ceramics. It is evidenced that the specimen derived from nanostructures shows a very homogenous and compact structure. The fracture is intergranular and the mean particle size is about 4 μm. This densified structure agrees well with the relative density of >97% measured for the material. The temperature dependence of dielectric constant ε_r and loss tangent, tan δ, at various frequencies (see ESI, Fig. S4†) were measured for the $KNbO_3$ ceramics derived from nanostructures. The Curie temperature T_c was 415 °C and the phase transition temperature T_2 from an orthorhombic symmetry to a tetragonal symmetry was approximately 220 °C. A sharp ε_r peak at T_c was obtained especially in higher-density KN ceramics, which indicates that such KN ceramics have good crystallinity. The frequency dependence of impedance on the (p) mode for the KN (see ESI, Fig. S5†) shows that this sample was approximately in the full poling state as judged by the maximum phase $\theta_{max} = 80.8°$ of impedance in the inductance region between the resonance and antiresonance frequencies; in particular, the electro-mechanical coupling factor k_p = 0.34, piezoelectric constant d_{33} = 105 pC/N and the mechanical quality factor Q_m = 216. A well saturated P–E hysteresis loop of $KNbO_3$ ceramics derived from nanostructures is shown in Fig. 3(b). The remanent polarization P_r and the coercive field E_c were 23 μC cm^{-2} and 8 kV cm^{-1} for KN, respectively. This result indicates that ceramics with a very homogenous and compact structure derived from nanostructures are effective in obtaining high-resistance specimens under a high electric field, and the easy reversals of polarization under dc bias are favored to the improvement of piezoelectric properties. Table 1 shows the piezoelectric properties of $KNbO_3$ systems cited from several previous reports. Until now, for the $KNbO_3$ ceramic system, Kakimoto *et al.*[23] reported the highest piezoelectric coefficient d_{33} = 98 pC/N in the $KNbO_3$–0.002 $LaFeO_3$ ceramics, which is lower than the value of 105 pC/N reported here. Besides, it should be noted that the specimens obtained by Kakimoto are based on the introducing of La and Fe into A and B sites of the perovskite structure, which changed the crystal lattice of $KNbO_3$.

In conclusion, single-crystalline $KNbO_3$ nanostructures have been prepared in a one-step molten salt synthetic reaction. Due to the good sintering ability of the nanostructures, "water-proof" $KNbO_3$ ceramics with a relative density >97% have been successfully prepared in a very limited temperature region by a conventional sintering method. These nanostructures possess excellent piezoelectric properties such as d_{33} = 105 pC/N and k_p = 0.34.

This work was funded by the National Natural Science Foundation of China (NSFC) (Grant No. 60601020), the Natural Science Foundation of Beijing (Grant No. 4072006), and the Science and Technology Development Project of Beijing Education Committee.

Notes and references

1 K. Nakamura, T. Tokiwa and Y. Kawamura, *J. Appl. Phys.*, 2002, **91**, 9272.
2 S. Wada, A. Seike and T. Tsurumi, *Jpn. J. Appl. Phys.*, 2001, **40**, 5690.
3 K. Nakamura and Y. Kawamura, *IEEE Trans.*, 2000, **47**, 750.
4 W. Aiying, P. M. Vilarinho, I. M. M. Salvado and J. L. Baptista, *J. Am. Ceram. Soc.*, 2000, **83**, 1379.
5 A. Magrez, E. Vasco, J. W. Seo, C. Dieker, N. Setter and L. Forro, *J. Phys. Chem. B*, 2006, **110**, 58.
6 C. H. Lu, S. Y. Lo and Y. L. Wang, *Mater. Lett.*, 2002, **55**, 121.
7 M. M. Amimi and M. D. Sacks, *J. Am. Ceram. Soc.*, 1991, **74**, 53.
8 K. Tanaka, K. Kakimoto and H. Ohsato, *J. Eur. Ceram. Soc.*, 2007, **27**, 3591.
9 I. Pribošič, D. Makovec and M. Drofenik, *Chem. Mater.*, 2005, **17**, 2953.
10 H. Birol, D. Damjanovic and N. Setter, *J. Am. Ceram. Soc.*, 2005, **88**, 1754.
11 I. Bilecka, I. Djerdj and M. Niederberger, *Chem. Commun.*, 2008, 886.
12 J. I. Park, Y. W. Jun, J. S. Choi and J. Cheon, *Chem. Commun.*, 2007, 5001.
13 Z. Y. Cai, X. R. Xing, R. B. Yu, X. Y. Sun and G. R. Liu, *Inorg. Chem.*, 2007, **46**, 7423.
14 Y. B. Mao, T. J. Park, F. Zhang, H. J. Zhou and S. S. Wong, *Small*, 2007, **3**, 1122.
15 G. Picard and P. Bocage, *Mater. Sci. Forum*, 1991, **73**, 505.
16 S. N. Mlondo, E. M. Andrews, P. J. Thomas and P. O'Brien, *Chem. Commun.*, 2008, 2768.
17 Y. D. Hou, L. Hou, M. K. Zhu and H. Yan, *Appl. Phys. Lett.*, 2006, **89**, 243114.
18 A. Banerjee and S. Bose, *Chem. Mater.*, 2004, **16**, 5610.
19 Y. M. Hu, H. S. Gu, X. C. Sun, J. You and J. Wang, *Appl. Phys. Lett.*, 2006, **88**, 193120.
20 U. Flueckiger and H. Arend, *J. Am. Ceram. Soc.*, 1977, **56**, 575.
21 K. Matsumoto, Y. Hiruma, H. Nagata and T. Takenaka, *Jpn. J. Appl. Phys.*, 2006, **45**, 4479.
22 H. Nagata, K. Matsumoto, T. Hirosue, Y. Hiruma and T. Takenaka, *Jpn. J. Appl. Phys.*, 2007, **46**, 7084.
23 K. Kakimoto, I. Masuda and H. Ohsato, *J. Eur. Ceram. Soc.*, 2005, **25**, 2719.
24 T. Wada, A. Suzuki and T. Saito, *Jpn. J. Appl. Phys.*, 2006, **45**, 7431.